A microfluidics device integrated with Surface Enhanced Raman Spectroscopy (SERS) for characterizing microplastics in aqueous samples

By

Mohsen Vahidi

Bachelor of Applied Science in Mechanical Engineering, Semnan University, 2010

Project Submitted in Partial Fulfillment of the

Requirements for the Degree of

MASTER OF ENGINEERING

In the Department of Mechanical Engineering

University of Victoria, Victoria, BC,

Canada

Declaration of Committee:

A microfluidics device integrated with Surface Enhanced Raman Spectroscopy (SERS) for characterizing microplastics in aqueous solutions

By

Mohsen Vahidi

Bachelor of Applied Science in Mechanical Engineering, Semnan University, 2010

Supervisory Committee:

Faculty Supervisor: Dr. Mohsen Akbari (Department of Mechanical Engineering)

Committee Member: Dr. Caterina Valeo (Department of Mechanical Engineering)

Abstract

Microplastic contamination is an emerging contaminant and concern that can be found all over the planet. These microplastics are often very tiny in size; therefore, they can readily pass though bedrock and infiltrate water bodies such as rivers, lakes, and seas. Whenever such environmental contamination occurs, the first step in order to address the issue is to characterize the contamination in order to define its origin. This project proposes a design of a microfluidic chip, which is integrated with a Surface Enhanced Raman Spectrometer to characterize microplastic particles in various aqueous solutions such as water. The proposed design is capable of sorting and collecting microplastics based on their size without any need for a membrane. It also has a flat architecture, which makes it easy to manufacture at a reasonable cost. SolidWorks was used for the computer aided design (CAD) of the microfluidic chip and COMSOL Multiphysics was utilized for computer aided engineering (CAE) calculation to verify the design. According to the calculations, this microfluidic chip is capable of size-based sorting of microplastics.

Keywords: Microplastics, Surface Enhanced Raman Spectroscopy (SERS), Microfluidics, Dean Flow, Inertial Sorting

Dedication

To my family who have been a constant source of support and encouragement throughout my academic journey. Their unwavering belief in my abilities and their unconditional love has been helping me to continue even in the darkest moments.

To my professors, colleagues, and friends whose guidance and expertise have helped shape my academic and professional development. Their passion for science and commitment to excellence has inspired me to strive for greatness.

Acknowledgements

I owe a great deal of gratitude to my supervisor, Dr. Mohsen Akbari, who was willing to give me the opportunity to pursue my research interests, for his guidance, support, and encouragement throughout this program. His expertise and dedication to teaching helped me to shape my research skills and learn that luck can sometimes play a role in scientific discovery. I am extremely grateful for his support, which has been crucial in the successful completion of this project.

I am also thankful to my supervisory committee members, Dr. Caterina Valeo for her insightful comments, constructive feedback, and valuable suggestions that have contributed to the overall quality of this work.

Additionally, I would like to express my sincere appreciation to the staff and faculty members in the Mechanical Engineering department for their unwavering support and guidance throughout the past few years.

Table of Contents

List of Figures

List of Acronyms and Units

MP	Microplastic
SERS	Surface Enhanced Raman Spectroscopy
PDMS	Polydimethylsiloxane
PBS	Phosphate Buffered Saline
NP	Nanoparticle
DC	Dean Cycle
CTC	Circulating Tumor Cell
RBC	Red Blood Cell
CAE	Computer Aided Engineering
CAD	Computer Aided Design
um	Micrometer
Pa	Pascal
m	Meter
m/s	Meter per Second
ug	Microgram
mL	Milliliter

Chapter 1. Introduction

1.1. Overview of the microplastic pollution

With the global population continuously growing, there is a significant need for the development of a new category of materials suitable for efficient production of goods in large quantities and short timeframes. This surge has led to the widespread adoption of plastic materials across various sectors such as textiles and packaging. Plastic encompasses a range of components like polyethylene (PE), polystyrene (PS), polyamide (PA), nylon, and other chemical compounds. However, the rapid proliferation of plastics has resulted in the uncontrolled disposal of plastic waste into the environment, ranging from microbeads found in personal care products to substantial plastic components [1].

Notably, even larger plastic items disintegrate into smaller particles over time due to natural factors like sunlight and moisture, exacerbating the negative impact as these particles decrease in size. In general, microplastics typically refers to any plastic particle ranging from 1 um to 5 mm in size. Due to their small size, microplastics pose significant threats to aquatic ecosystems [2].

Eriksen et al.'s [3] estimation in 2014 revealed a staggering reality about the state of the global oceans; over 5 trillion pieces of plastic, collectively weighing nearly 270,000 tons, were dispersed across marine ecosystems.

There is strong evidence stating that these microplastics can enter the food chain when they are swallowed by sea creatures and end up in human food products. Even in some areas, microplastic particles are reported in air as well as rain. Moreover, microplastic particles have even been observed in air samples from certain regions with high concentration of contamination [4].

1.2. Microplastic pollution origins

The sources of microplastics are multifaceted, originating from various human activities. Large plastic items discarded in natural environments undergo degradation processes, fragmenting into smaller pieces over time due to exposure to sunlight, mechanical forces, and chemical reactions. Additionally, the use of microbeads in cosmetics and personal care products introduces microplastics into the environment. Furthermore, the disposal of laundry wastewater, primarily containing microfibers shed from textiles during washing, constitutes another significant source of microplastic pollution.

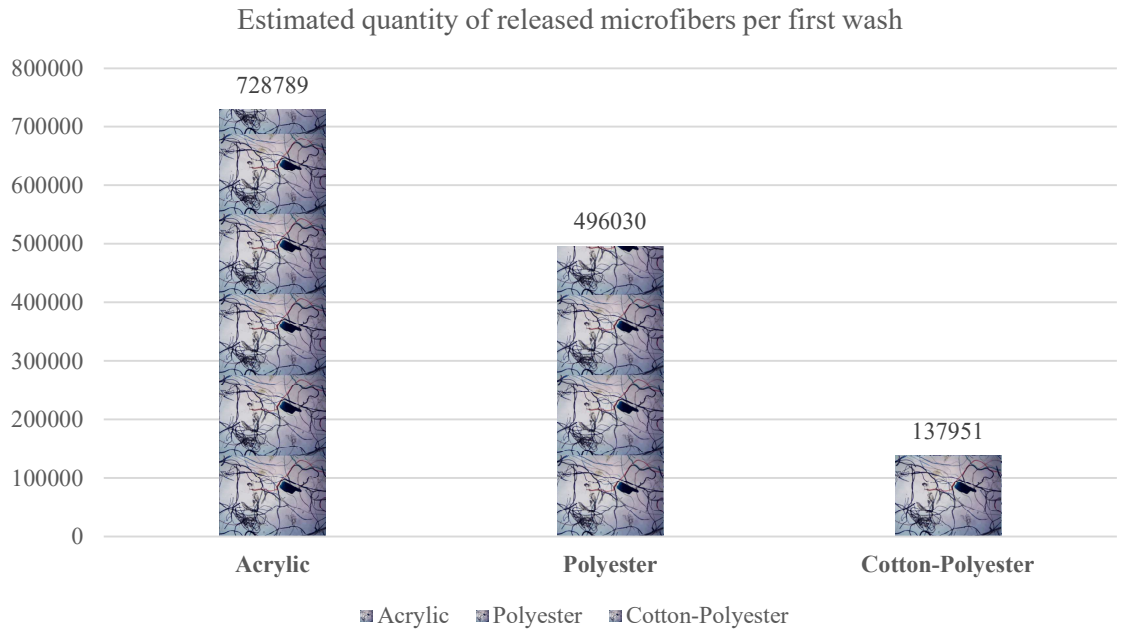

Figure 1: Estimated quantity of released microfibers per wash

Figure 1 shows a study published in the Marine Pollution Bulletin in 2016 in which authors meticulously examined the shedding of microfibers from different fabric types during their initial wash cycles, with acrylic fabrics demonstrating a particularly high release of microfibers (over 700,000 pieces of microfiber during the first wash) [5].

1.3. Microplastics and marine environment

Due to their tiny size, microplastics can simply pass through bedrock and infiltrate water resources and end up finding their way to seas and oceans. Therefore, marine life turned into the major victim of this contamination and the major pathway for microplastics to find their way into the human food basket. Cole et al. [7] employed advanced fluorescent imaging techniques to investigate the ingestion of microplastic particles by specific species of zooplankton residing in the northeast Atlantic (See figure 2). This microscopic exploration revealed the pervasive presence of microplastics within the planktons' body

which are the foundational levels of marine food chain in the ocean, indicating the widespread distribution of plastic pollution in marine environments and its potential impacts on marine life.

Figure 2: Microplastics ingested by zooplanktons, imaged using fluorescent imaging (Adapted from [7] and used with publisher permission)

In a parallel study conducted by Garnier et al. in 2019 [8], the focus shifted to the digestive systems of wild tropical fish inhabiting Moorea Island in French Polynesia, a remote region in the Pacific Ocean. This investigation unveiled a diverse array of microplastics ingested by these fish, highlighting the extent of microplastic contamination even in isolated marine ecosystems.

1.4. Characterizing techniques

When it comes to environmental contaminations, finding the source becomes challenging and microplastics are no exception. Various techniques have been discussed in the literature for characterizing microplastics, however an efficient method should be capable of providing fast response, have accuracy and be easy to use and have high capability of continuous analysis, etc.

Identification methods

In general, microplastics refers to any plastic particle smaller than 5 mm in size. Microplastics are divided into two main categories. First, there are microplastics that are intentionally engineered such as microbeads which are widely used in cosmetics and toothpaste. This group of microplastics is also known as primary microplastics. The second category is microplastics that are generated by fragmentation of large plastic pieces littered in the environment. Either of these two categories will be challenging to remove from the environment as soon as they contaminate an area. They can pose a threat to both humans and living organisms. Their adverse impact gets worse as their size gets smaller, since a smaller size makes it easier to infiltrate water bodies and end up in living organisms.

Here is when monitoring and characterizing microplastics becomes important and that's because it helps scientists to identify the source that is spreading microplastics into the environment. Pollution status, identifying spots with high levels of contamination and realizing historical trends to name a few are other benefits of characterizing microplastics.

Generally, analytical methods of characterizing microplastics start with sampling, then extracting, isolating, identifying and quantifying or classifying particles. Most conventional methods were dependent on visual sorting. Those techniques were only practical for large particles (between 1 to 5 mm) since they were mostly reliant on using the naked eye. However, the smaller the microplastics are, the greater their environmental impact will be, and it necessitates the demand for implementation of other analytical techniques for identification of smaller particles.

As a result, characterizing microplastics based on their size, shape and polymer type becomes a complex process that requires exploitation of typically more than one analytical method. These analytical methods usually consist of a physical characterization, which is mostly done using microscopy tools, and a chemical characterization, which is done using spectroscopy methods. Each of these techniques offers advantages while it poses limitations as well. In general, all identification methods for microplastics fall into the following categories described below.

1.4.2. Visual inspection

There are a wide range of plastic particles that are distinguishable using visual methods. One advantage of this method is that it is capable of classifying microplastics based on their color and texture. This method is fast and simple and requires a minimum level of skillset to be performed. However, there is always a risk of mistaking organic particles with microplastics [9], [10].

1.4.3. Microscopy

Optical microscopy techniques are mostly applicable for particles of hundreds of micron size. By using this technique, more information can be derived about the surface texture and structure of the particle. It also reduces the risk of mistaking organic matters rather than microplastics [11].

Additionally, scanning electron microscopy (SEM) techniques also fall under this category. SEM imaging offers high resolution images of the surface texture of the particle and enables scientists to distinguish microplastics from organic matter. Yang et al. [12]

developed a method that allows scientists to perform in situ SEM imaging on samples of liquid form. An energy dispersive X-ray device (EDS) can also be integrated to the SEM in order to provide detailed information about the elemental composition of the particle. However, this technique poses some limitations such as being expensive, requiring high degree of skills and limited volume for inspection [13], [14], [15].

1.4.4. Fourier Transform Infrared (FTIR) spectroscopy

Fourier Transform Infrared spectroscopy (FTIR) is a method used to obtain an infrared spectrum of absorption or emission of any form of material including solid, liquid, or gas. An FTIR spectrometer is capable of collecting high-resolution spectral data over a wide spectral range. It uses modulated infrared energy to investigate a sample. The infrared light in this method is absorbed at a specific frequency, which is proportionate to the atom to atm vibrational bond energies in that molecule. When the bond energy and the energy of the infrared light are identical, the bond absorbs that energy. Different bonds in a molecule vibrate at different energies and therefore they are capable of absorbing different wavelengths of infrared radiation. The frequency and intensity of the absorption bands contribute to the overall spectra and generates a unique characteristic for the molecule, which helps to identify the structure of molecules and the composition of the sample. That's because FTIR creates a signal specific to that type of bond. FTIR is widely used in analyzing polymer science and chemical engineering. Microplastics particles are nothing but carbon-based polymers; therefore, FTIR offers ample opportunity to utilize this technique [16].

1.4.5. Raman spectroscopy

Raman Spectroscopy has been utilized in several published research works to identify microplastics [17], [18]. In this technique, the laser beam hits the microplastic particle and generates multiple frequencies of back-scattered light depending on the molecular structure of the sample. One of the advantages of this method is that it is contact-less and non-destructive for the sample, therefore, the sample can be utilized for further investigation and analysis afterwards. The minimum size of the interrogated particle in this method depends on the laser beam diameter. The smaller the laser beam, the smaller the particles that can be inspected. It can even go down to a few micrometers in size. However, in order to have an accurate analysis with such a tiny laser beam, particles should be all aligned in a small area of interest. Therefore, liquid samples require focusing prior to scanning by this technique. Focusing is going to be discussed extensively in the next sections of this project.

History

Raman spectroscopy is very similar to infrared spectroscopy in which scientists look at the vibration of molecules. As we know from basic chemistry, all molecules are made of atoms which are held together by chemical bonds. These chemical bonds are like springs and can vibrate. For instance, a water molecule is made of one oxygen atom and two hydrogen atoms which are linked together by hydrogen bonds. These bonds can vibrate either symmetrically or anti-symmetrically or bend.

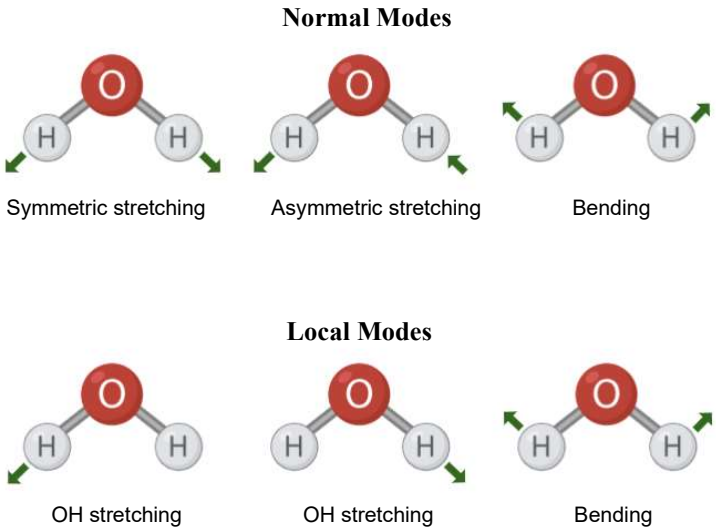

Figure 3: Vibration modes of a water molecule

These bonds can vibrate either symmetrically or anti-symmetrically or bend as it is shown in figure 3. Each of these vibrating modes corresponds to a certain amount of energy, which in turn corresponds to a different wavelength of infrared light and subsequently creates a spectrum. Analyzing the spectrum enables scientists to find out what compound exists in the analyzed sample.

From this standpoint, Raman Spectroscopy is very similar to Infrared Spectroscopy. However, there are a few fundamental differences. First and foremost, Raman spectroscopy utilizes laser beam instead of infrared. One of the other differences is that water does not show up in Raman Spectroscopy, or even if it shows up, it appears as a very weak shift in the spectrum. This makes Raman Spectroscopy a perfect tool for analyzing samples in aqueous form such as environmental samples [19].

An improvement to Raman Spectroscopy was first introduced by researchers in the 1970s. They realized that by adding metallic collides next to the analyte, a huge shift will occur in Raman shists that enhances resolution of the spectroscopy. Surface-Enhanced Raman Spectroscopy (SERS) is a powerful analytical technique that enhances the Raman scattering of molecules adsorbed on rough metal surfaces or nanostructures. The discovery of SERS dates back to 1974 when Martin Fleischmann and his colleagues observed unexpectedly strong Raman signals from pyridine molecules adsorbed on a rough silver electrode [20]. Initially, this enhancement was attributed to the increased surface area of the rough electrode. However, in 1977, two independent research groups provided a deeper understanding, attributing the enhancement to electromagnetic and chemical mechanisms [21], [22]. These findings laid the foundation for the rapid development and widespread adoption of SERS in various scientific fields.

SERS Mechanism

The mechanism of SERS involves two primary enhancement effects: electromagnetic enhancement and chemical enhancement.

I. Electromagnetic Enhancement: This is the dominant mechanism, contributing to most of the signal enhancement. It arises from the excitation of localized surface plasmons in metal nanoparticles (typically gold, silver, or copper). When the incident light interacts with these nanoparticles, it induces collective oscillations of conduction electrons, creating an enhanced electromagnetic field at the nanoparticle surface. This field can increase the Raman scattering signal by several orders of magnitude (10^4 to 10^6 times).

II. Chemical Enhancement: This mechanism contributes less to the overall enhancement but is still significant. It involves the formation of charge-transfer complexes between the adsorbed molecules and the metal surface. This interaction can alter the polarizability of the molecules, leading to an increase in Raman signal intensity. Chemical enhancement typically accounts for a factor of 10 to 100 in signal amplification [23].

Strengths of SERS

Surface-Enhanced Raman Spectroscopy (SERS) is renowned for its high sensitivity, which allows for the detection of single molecules in certain scenarios. This exceptional sensitivity makes SERS invaluable for trace analysis in diverse fields, including environmental monitoring, food safety, and medical diagnostics. Additionally, SERS provides molecular specificity through the unique molecular fingerprints in Raman spectra, enabling precise identification and characterization of analytes. The non-destructive nature of SERS preserves sample integrity during analysis, making it suitable for delicate or valuable samples. Furthermore, the versatility of SERS allows it to be applied to a wide array of molecules and materials, including biological samples, chemicals, and nanomaterials, facilitating rapid and real-time data acquisition [24].

Drawbacks of SERS

Despite its many advantages, SERS has some notable drawbacks. Achieving reproducible SERS signals can be challenging due to inconsistencies in substrate preparation and the uneven distribution of nanoparticles, which can affect signal intensity and reliability. The stability of SERS-active substrates is another concern, as they may degrade over time or

under certain environmental conditions, potentially compromising their performance. Additionally, interpreting SERS spectra can be complex, particularly for mixtures or unknown samples, necessitating advanced data analysis techniques and expertise. The reliance on noble metals like gold, silver, and copper for substrates also limits the range of applications, as these materials may not be suitable for all analytes or conditions [25].

Applications of SERS

SERS has found a wide range of applications across various fields due to its sensitivity and specificity. In biomedical diagnostics, SERS is used to detect biomolecules, pathogens, and disease markers, offering potential for early diagnosis and personalized medicine. Environmental monitoring benefits from SERS's ability to detect pollutants and contaminants at trace levels, aiding in efforts to protect the environment and ensure regulatory compliance. In the food safety sector, SERS is employed to identify contaminants, additives, and adulterants in food products, ensuring quality and safety for consumers. The chemical and pharmaceutical industries utilize SERS for analyzing complex mixtures, monitoring reactions, and conducting quality control [26].

1.5. Nanoparticles

Surface-enhanced Raman spectroscopy (SERS) is an exceptionally sensitive method that boosts the Raman scattering of molecules when they are placed on certain nanostructured materials. By utilizing plasmon-mediated amplification of electric fields or chemical enhancement, SERS enables the identification of the unique structure of trace analytes with low concentrations.

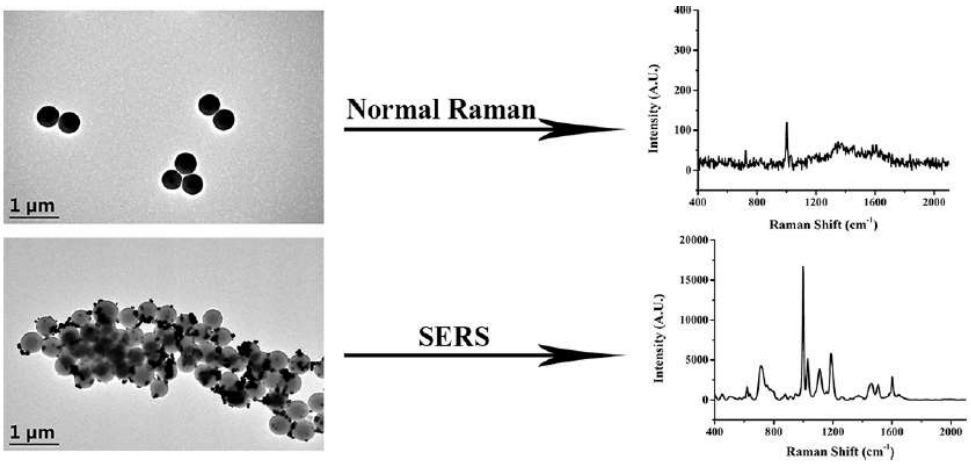

Figure 4: Effect of silver nanoparticles labelling on SERS shift (Adapted from [27] and used with publisher permission)

As it is shown in figure 4, Lulu Lv et al. [27] compared SERS with regular Raman spectroscopy and stated that using SERS, they obtained a 40,000 times enhancement in their Raman shift. They declared that by using this method they could detect microplastics of 100 nm size at the low concentration of only 40 ug/mL.

Gold and Silver colloids are two widely used nanoparticles in SERS applications, each of which offer some advantages while it may have some drawbacks too. For instance, silver atoms have higher reactivity compared to gold atoms which makes it more difficult to create monodisperse nanoparticles in a reproducible process [28]. However, Abalde-Cela et al. [29] who made a comparison between the effect of Au and Ag nanoparticles on SERS results stated that silver nanoparticles create a 10 to 100 times larger shift in SERS spectrum which increases the resolution drastically. Conversely, Gold colloidal can be generated more homogenously but the SERS shift, they create is not as large as that of silver colloidal.

1.6. Flow focusing

Sorting is one of the primary applications of microfluidics. It is widely exploited for sorting cells and biological particles in drug development and cancer treatments. Sorting techniques are categorized into two main groups: active and passive. Active sorting methods refer to microfluidic chips that utilize an external source of energy to perform the separation of various particles. In contrast, passive sorting techniques take advantage of variations in geometry to create secondary flows within the main flow using hydrodynamic forces. This passive method is also referred to as hydrodynamic focusing in the published literature.

Various geometries have been introduced so far, which are all capable of generating secondary flow. One way to categorize these geometries is to divide them into two groups of straight and curved channels. In straight channels, the lift forces, which are introduced by the shear stress as well as the wall, will counteract each other and as a results exert a force that makes the particles within the flow to be inclined towards the center of the exterior wall of the curvature, which is larger [30], [31], [32], [33]. Zhou et al. [34] modulated the microchannel aspect ratio in order to induce inertial lift force within the flow. Later on, in another research work, they demonstrated how expansion regions along the flow in straight microchannels creates micro vortices and causes lift force induced by the channel walls.

Lee et al. [35] discovered that by sending the flow through a series of contraction and expansion zones, they can create a secondary flow and focus the sample flow in the middle of the channel surrounded by the sheath flow. The dimensions of the channel they designed

were in the order of tens to hundreds of microns; therefore, the same concept can be extended to other microfluidic device designs.

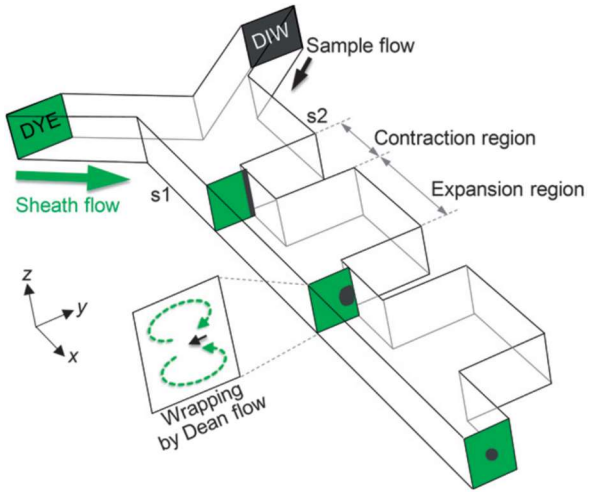

Figure 5: Hydrodynamic focusing using straight microchannels (Adapted from [35] and used with publisher permission)

As it is shown in figure 5, Lee et al. [35] discovered that by increasing the number of contraction-expansion regions, the position of the sample flow can be shifted from one side and be brought to the center of the channel.

Fluid dynamic gets more complicated when channel geometry includes curvatures since it develops secondary flow causing the formation of Dean flow, which plays a crucial role in manipulating microparticles suspended in the flow. This concept is the predominating idea behind most of the microfluidic systems that are designed to be used in particle separation applications. This is simply because of the counter-rotating vortices that are generated in the flow due to this secondary flow [36]. These vortices are created as a result of a balance between shear-induced lift forces and wall-induced lift forces.

Dean flow

In 1927, Dean performed an extensive analysis on the dynamics of flow in microchannels and discovered that in curved pipes with a circular cross-section, the laminar Poiseuille flow experiences a centrifugal force [37]. This force disrupts the parabolic profile of the laminar or primary flow, causing the peak velocity point to shift from the center of the channel to the concave wall. This shift creates a steep velocity gradient between the maximum velocity point and the concave wall. Needless to say, convex wall points out to the inner channel wall and concave wall points out to the outer channel wall. The resulting steep gradient increases the pressure, and the local velocity near the walls becomes insufficient to fully counterbalance this pressure gradient. This imbalance, known as Dean instability, leads to fluid recirculating as vortices that move from the center of the channel towards the outer wall and then back to the center to balance the pressure gradient.

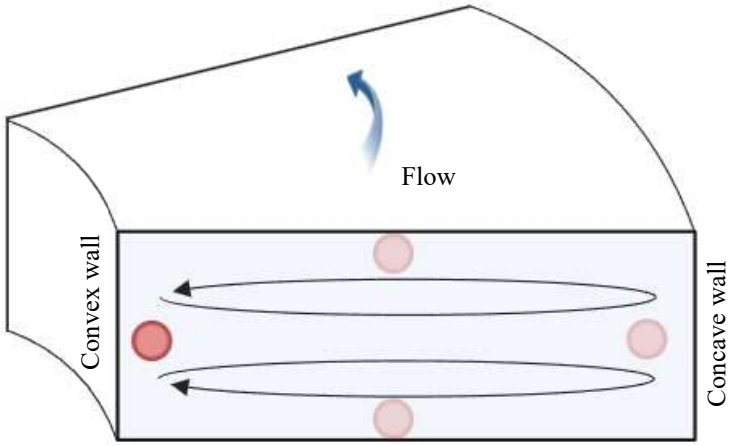

Figure 6: Counterrotating vortices formed in curved microchannel

As seen in figure 6, the imbalance in pressure and velocity gradients due to Dean instability leads to the formation of vortices, also known as secondary flow, which is characterized by a non-dimensional number called the Dean number (De). De serves as a control

parameter for the secondary flow, directly indicating the Dean force or the force caused by the secondary flow in curved channels, and it can be calculated from equation 1 [37].

$$De = Re\sqrt{\frac{D_h}{2R}} \quad (1)$$

Where Re is the Reynolds number, D_h is the hydraulic diameter, and R is the curvature radius. This equation states that the strength of the dean force depends on the flow speed, channel cross section and the spiral characteristics. The Dean number is an indicator of the relative importance of centrifugal forces (due to curvature) compared to viscous forces in the fluid flow.

From this equation, a straight channel can be assumed as a channel with an infinite curvature radius. In such channel, there will be no secondary flow, and the De will be zero.

The current understanding of Dean flow dynamics in spiral micro-channels relies on the concept of two counter-rotating vortices. This concept is somewhat validated by various fluid mixing studies, which, despite being comprehensive, are mainly numerical and typically limited to low Reynolds numbers, $Re < 20$ [38]. However, at higher Reynolds numbers, this assumption of two counter-rotating vortices fails because the actual focusing positions of cells deviate from the predicted ones [39].

Dean flow applications in particle separation

Hou et al. [40] utilized dean flow phenomena and designed a high throughput microfluidic device capable of performing size-based separation on circulating tumor cells. It facilitates migration of the circulating tumor cells across the channel cross section using inertial

forces. This device has several advantages over existing methods. First of all, it is capable of processing and sorting large volumes of clinical samples at an astonishing rate of approximately 3 liters per hour. Moreover, thanks to its channel geometry and dimensions, authors claimed that it is free of any risk related to blood coagulation which makes it superior over the competitors. They conducted a clinical trial on their invented device and verified through correlation of their numerical calculations with experimental results.

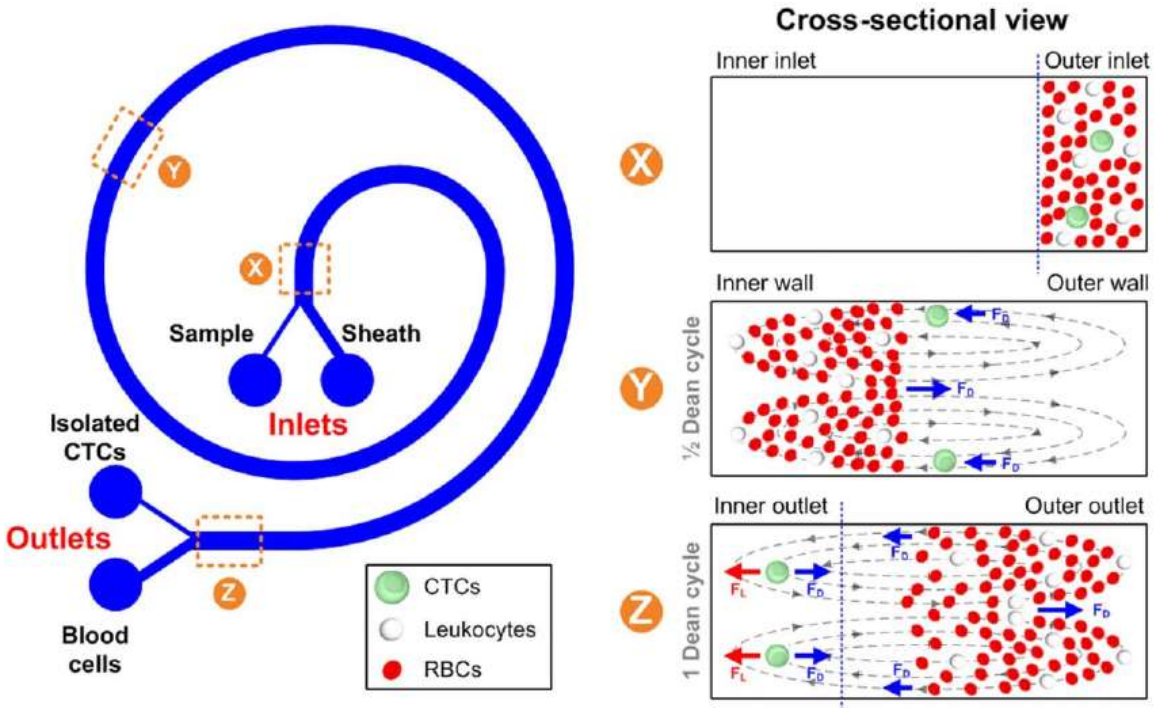

Figure 7: Curved microfluidic channel for size-based separation of particles (Adapted from [40] and used with publisher permission)

Figure 7 shows how CTCs (Circulating Tumor Cells), which are larger than RBCs (Red Blood Cells) and leukocytes, migrate across the channel cross-section during a Dean cycle and aggregate at the inner side wall of the spiral (convex wall), while RBCs and leukocytes are collect on the outer side wall of the spiral (concave wall).

Chapter 2. Method and results

2.1. Proposed design for microfluidic chip integrated with SERS

As shown in figure 8, the suggested design comprises a Y-junction in the beginning. An aqueous sample which is suspected of carrying microplastics enters one side and silver nanoparticles are introduced from the other side. After combining both flows, they go through an array of consecutive contraction and expansion regions. This creates a secondary flow that helps the stream of specimen to get separated from the wall and gets focused in the middle of the cross section. This creates the ideal condition for scanning the flow using the laser beam.

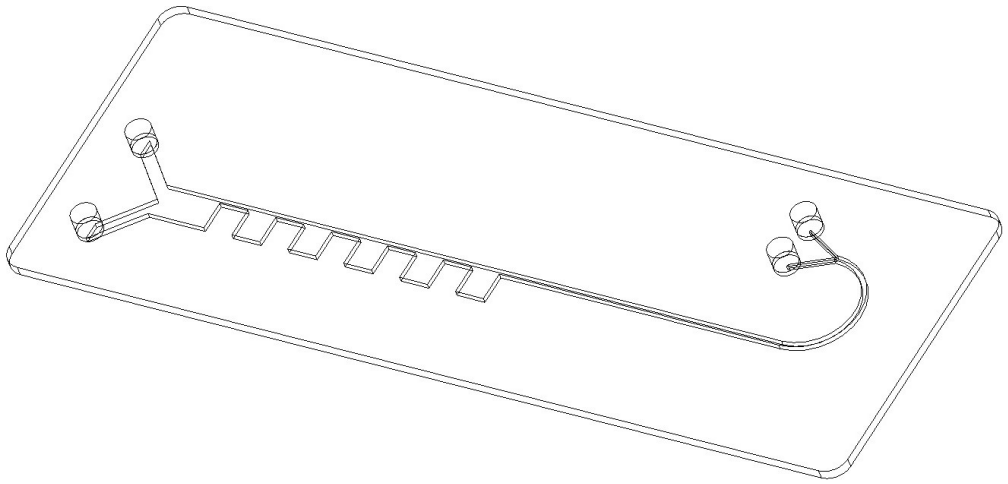

Figure 8: The proposed design for microfluidic chip

After scanning, flow goes through a curved channel that facilitates inertial sorting of the microplastics based on their size and provides the opportunity of further investigation on the pollutant origin.

2.2. Microchannel detail design selection process

To optimize the number of iterations required for efficient flow focusing and particle sorting, an attempt was made to reverse-engineer most parameters of the microfluidic device from values reported in relevant published literature. The channel width and height were selected in a manner consistent with the design proposed by Lee et al. [35]. Based on CAE results, these dimensions were found to be promising, despite having been originally designed for a different fluid property (blood). In order to determine the optimum number of contraction and expansion zones for aligning particles at the center of the channel, a simulation was conducted using COMSOL Multiphysics.

The design of the curved section of the microfluidic device was inspired by the work of Hou et al. [40], in which a 630-degree curvature microchannel was employed for particle sorting of blood samples. For the first iteration of the simulation, the same geometry was used for particle sorting; however, the results were unsatisfactory, as all particles accumulated in the same corner of the microchannel after traversing the curvature. Nevertheless, particle tracking within the microchannel indicated that the largest particles could be extracted from the flow after the first 180-degree curvature. As a result, the curvature of the microfluidic device was modified to a 180-degree curved channel with a constant cross-section.

2.3. Channel dimension and relevant calculations

The Microchannel consists of a rectangular cross section which is 50um in height and 350um width in the entry zone of the microchannel. The hydraulic diameter calculation of such channel will be as follows. If we assume "a" as height and "b" as width, then the hydraulic diameter calculation will be as follows:

$$Hydraulic\ Diameter\ (D_h) = \frac{4 * (a.b)}{2 * (a + b)} = 8.75 * 10^{-5}\ (m) \quad (2)$$

A flow of 50 mL/h would translate into the flow velocity of 0.79 m/s and the Renolds number calculations will be as follows:

$$u = \frac{Q}{A} = \frac{1.38 * 10^{-9}\ \ (m^3/sec)}{1.75 * 10^{-8}\ \ (m^2)} = 7.9 * 10^{-1}\ (m/\text{sec}\ ) \quad (3)$$

$$Re = \frac{\rho\ .\ u\ .D_h}{\mu} = 73 \quad (4)$$

Where Q is the flow rate, A is the channel cross section, u is the flow velocity, ρ is the seawater density and μ is seawater dynamic viscosity.

Considering the low Reynolds number, it can be concluded that the flow regime is laminar throughout the microfluidic channels. Therefore, pressure drop for such flow can be calculated by the following equation.

$$\Delta P = \frac{128 * \mu * L * Q}{\pi *\ D^4} = 9309\ (Pa) \quad (5)$$

This pressure drop should be taken into account for proper pump selection.

Eventually, having the Reynolds number of 73 and spiral curve of 4 millimeters, the Dean number (De) calculations will be as follows.

$$De = Re\sqrt{\frac{D_h}{2R}} = 76 \quad (6)$$

2.4. Flow driving force

Flow is forced into this microfluidic chip using a syringe pump. These pumps are affordable, fairly simple to operate and provide even pressure consistently and in a controlled manner without undesirable pulsations. Syringe pumps also offer other advantages for this particular application, because the aqueous sample can be stored in the syringe and then fed into the microfluidic chip gradually until the Spectroscopy is done, and results are obtained. Needless to say, that water which is the main media and flows through this microfluidic chip is considered a Newtonian fluid. It means that its viscosity is assumed to be constant with varying shear rates.

2.5. Y junction

Y junctions are critical components in microfluidic devices, and they are referred to as the section of the microfluidic device in which either two channels merge and form one channel or a single channel split into two. The bifurcation angle at these junctions significantly influences the fluid dynamics within the microchannels. Understanding these effects is crucial for optimizing microfluidic designs for specific applications.

Pressure drop across any type of Y junction is a critical factor influencing fluid flow. As the bifurcation angle increases, pressure drop tends to increase due to the higher resistance encountered by the fluid. At smaller angles, flow splits more smoothly, resulting in a relatively lower pressure drop. In contrast, larger angles create sharper turns for the fluid, causing greater turbulence and energy dissipation, which manifests as a higher pressure drop.

Velocity distribution within the microchannels also varies with the bifurcation angle. Smaller bifurcation angles result in more uniform velocity profiles in the daughter channels, promoting laminar flow conditions. As the bifurcation angle increases, the velocity profiles become more skewed, with higher velocities near the outer walls of the channels due to the centrifugal forces acting on the fluid. This can lead to increased shear rates and potential flow instability at larger bifurcation angles [41].

Frictional losses in microfluidic channels are influenced by the bifurcation angle due to the changes in flow direction and velocity gradients. Smaller bifurcation angles tend to have lower frictional losses as the flow remains more streamlined. In contrast, larger angles induce greater frictional forces as the fluid navigates sharper turns, leading to higher energy losses and potentially affecting the efficiency of the microfluidic processes [42].

2.6. Dean flow and flow focusing within contraction-expansion array

Raman spectrometer laser beam spot size ranges from half a micron to 10 microns depending on the application and laser beam characteristics. Therefore, to have an accurate

scanning of the specimen the particles should be focused in the middle of the channel ideally. To achieve this goal, an array of consecutive expansion and contraction chambers are designed along the pass for the flow. This series of expansion and contractions causes a secondary flow within the channel that separates the specimen from the side wall and brings it in the middle of the channel. COMSOL Multiphysics ® version 6.0 was used to visualize this effect.

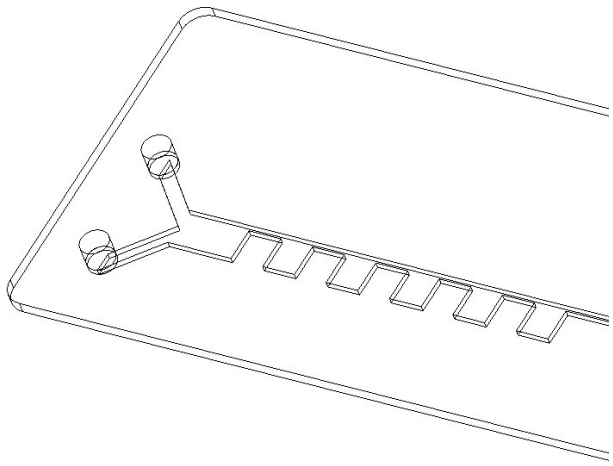

Figure 9: Array of consecutive contraction and expansion zones in the suggested design of the microfluidic device

As shown in figure 9, five consecutive zones of contraction and expansion are incorporated in this microfluidic chip design. Despite introduction of the sample from the lower inlet and PBS (Phosphate Buffered Saline) introduction from the upper inlet, the sample flow starts to depart from the side under the influence of the secondary flow. In fact, as the mixture of the sample flow and the PBS pass through the contraction and expansion zones a secondary flow is created which results in separating the sample flow from the side wall and getting it focused somewhere on the middle of the channel. This creates the ideal situation for the particles within the sample to be scanned by the Raman Spectrometer. Lee et al. [35] demonstrated these phenomena by introducing PBS and a die replicating red

blood cells from two different inlets of a similar array of consecutive expansion and contraction zones. Figure 10 shows how after passing through a certain number of zones, the die flow departs from the S2 wall and centers in the middle of the channel.

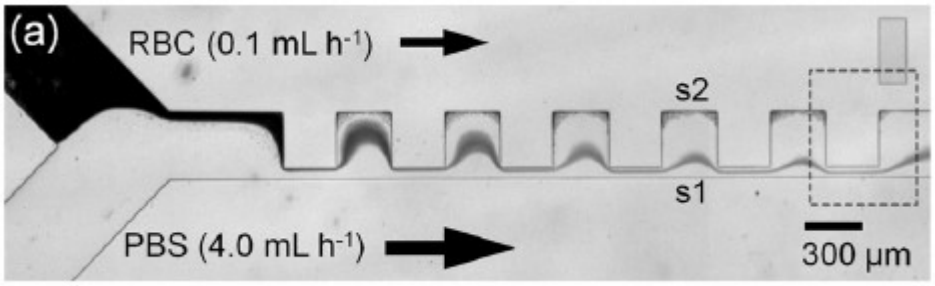

Figure 10: Die flow focusing in the middle of the channel (Adapted from [35] and used with publisher permission)

By running simulations, they realized that there is a correlation between the number of the expansion-contraction zones with the distance of the die from the side wall. Additionally, they backed up this finding by experiment. According to what is shown in figure 11 plotted by Lee et al. [35], the sample flow ideally focuses in the middle of the channel after passing through four to five expansion-contraction zones.

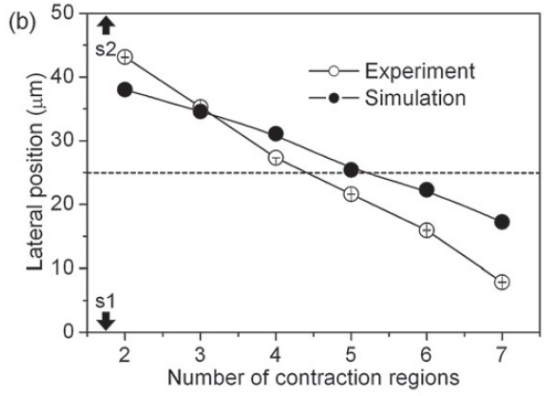

Figure 11: Effect of contraction zones quantity on lateral position of the flow (Adapted from [35] and used with publisher permission

As shown in figure 12(A), this geometry was transplanted into the microfluidic chip design which is the subject of the project. Similarly, an aspect ratio of 1:7 was selected for the

design of contraction and expansion regions. 3D simulations of the suggested design show how the secondary flow forms right after passing the expansion zone when the flow just enters the contraction area (see figure 12(B)). Passing flow through five sets of contraction and expansion regions shows promising results according to the simulations, as maximum of the secondary flow pointed towards center of the channel.

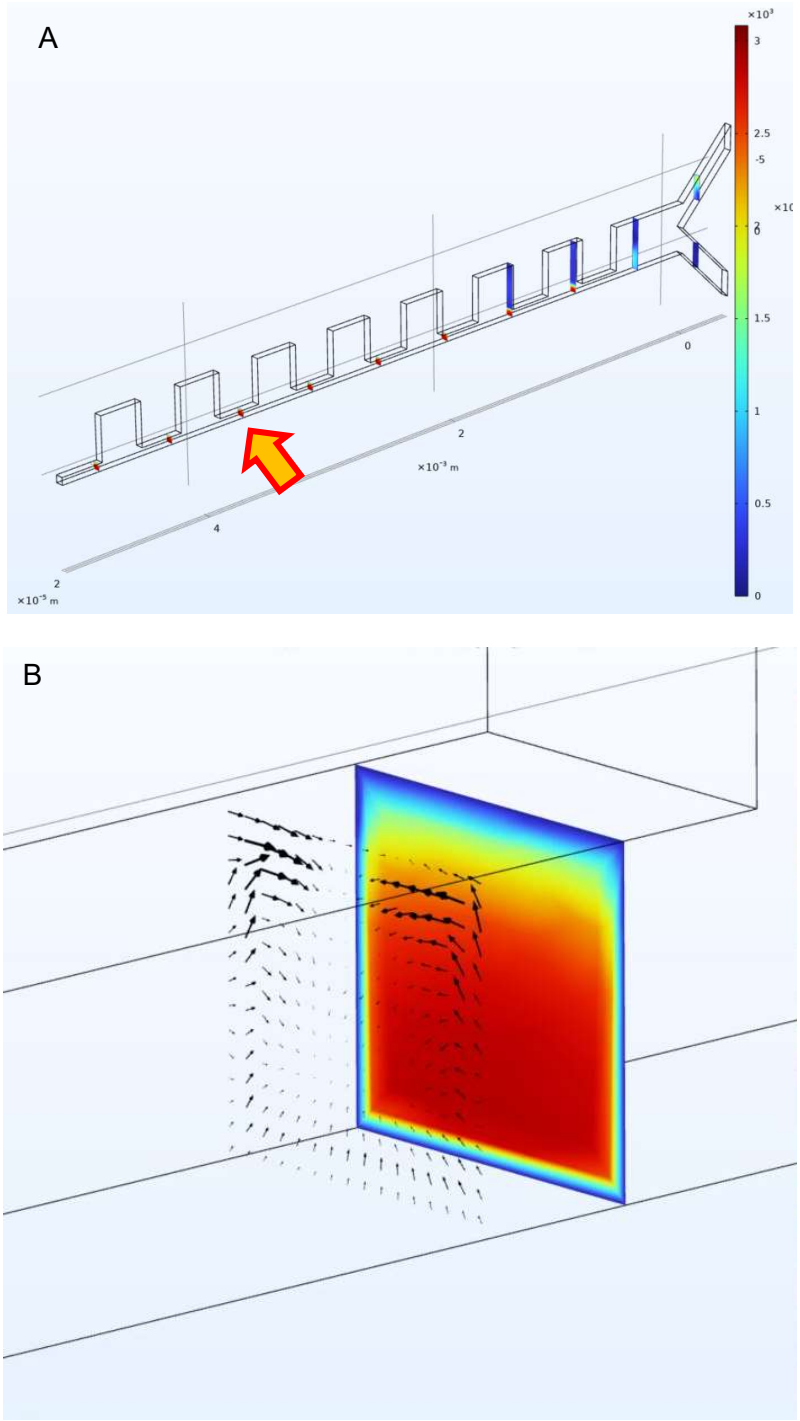

Figure 12: (A) Optimum cross section in terms of having maximum concentration of the sample in the middle of the cross section, (B) Secondary flow formed at the beginning of the contraction zone after passing five sets of contractions and expansions

2.7. Particle tracking

COMSOL Multiphysics ® version 6.0 was used for the particle tracking within the designed microfluidic chip. Seawater is defined as the medium flowing through the microfluidic channel since this device is going to be used for analyzing microplastics within the waterbodies.

In general, the governing regime is assumed to be laminar flow considering the flow rate and channel dimensions. The inlet flow speed is set at velocity field value and the outlet pressure is set at atmospheric pressure (0 atm gauge pressure).

The initial design for the spiral section comprised a 630˚ spiral as it can be seen in figure 13. Simulation showed that in such spiral channel, the larger particles (shown with a red arrow in figure 13) due to their higher inertia are less affected by the Dean force and therefore they tend to stay longer in their initial position as the flow goes down the spiral. Conversely, smaller particles that are lighter and have relatively less inertia, first move towards the convex wall (inner wall) of the channel during the first 180˚ of their travel through the microchannel. However, when the flow goes further into the spiral, the smaller particles then move back towards the concave wall (outer wall) again under the influence of the Dean flow. This lateral migration of the floating particles between the inner and outer wall is what Hou et al. mentioned as Dean Cycle (DC) in their work [40]. Therefore, for an efficient separation of the smaller particles from the larger ones, they should be bifurcated somewhere down the spiral where both particles are well departed and are on the opposite sides of the channel wall.

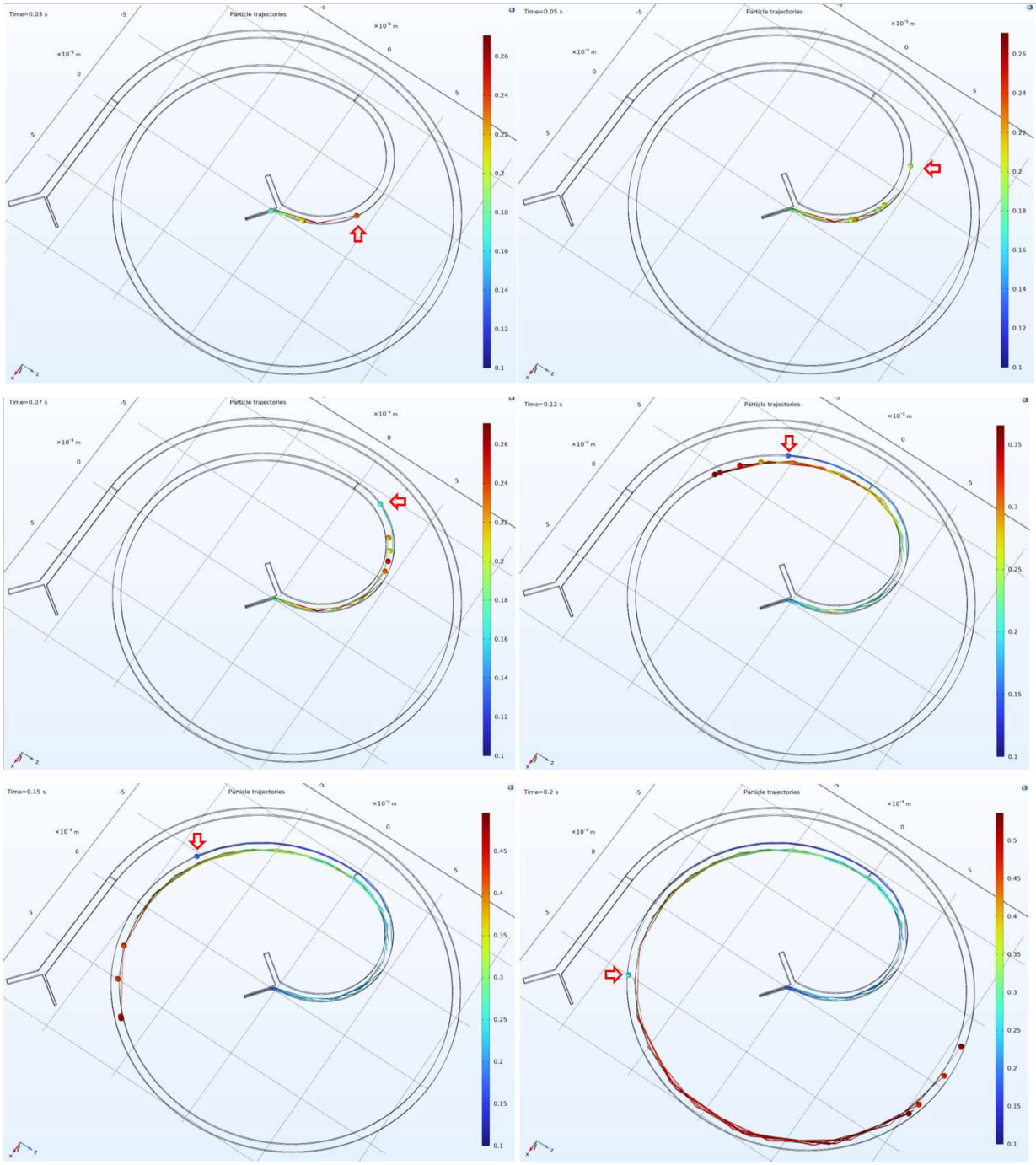
Time=0.03 s
Particle trajectories
Time=0.05 s
Particle trajectories
Time=0.07 s
Particle trajectories
Time=0.12 s
Particle trajectories
Time=0.15 s
Particle trajectories
Time=0.2 s
Particle trajectories

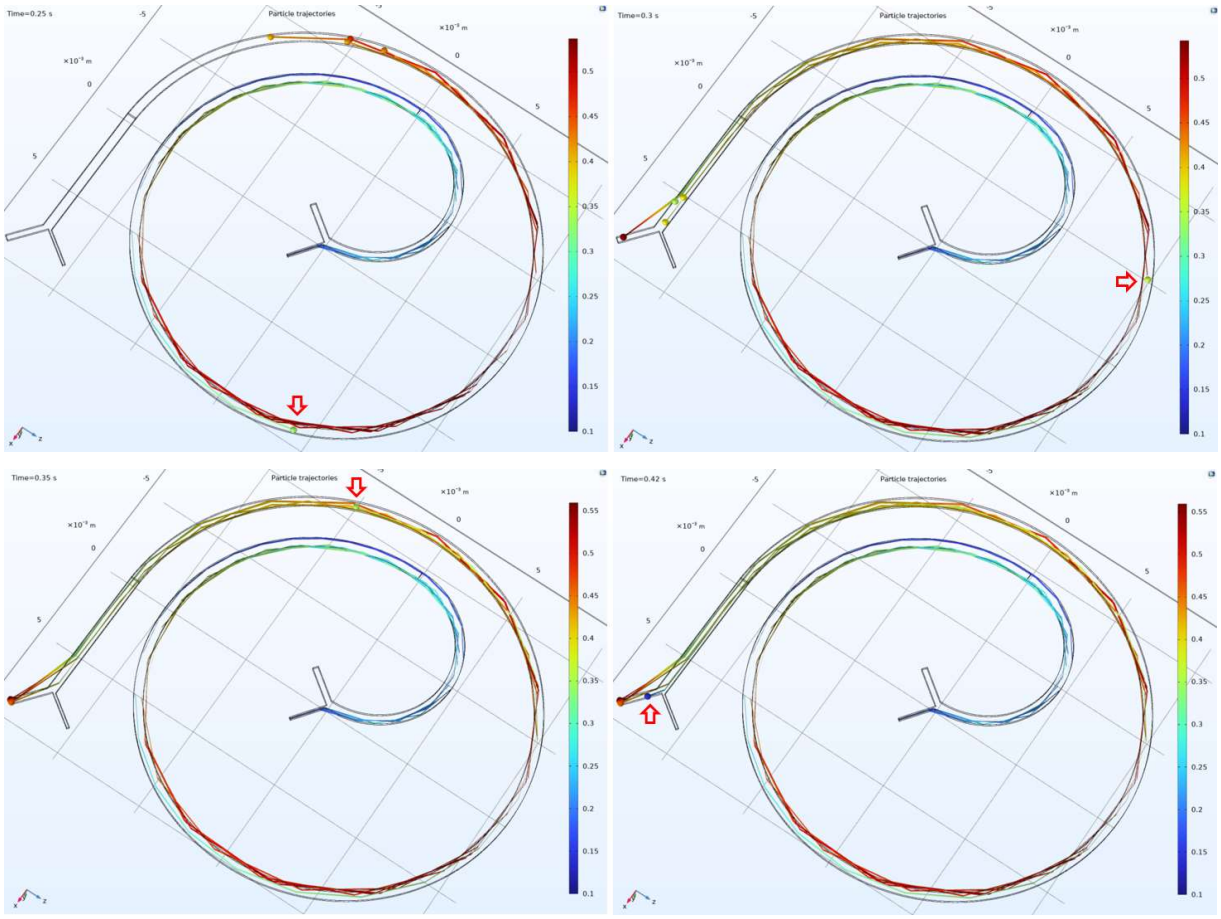

Figure 13: A complete Dean Cycle for a certain floating particle at relatively higher size and weight within the cluster

The second design is engineered based on the obtained results from the previous design and it only contains a 180˚ degree microchannel that would separate the larger particles from the other ones.

In the second design, three different particles of various sizes (6, 10, and 20 micrometers), mimicking the microplastics within the water were released at the inlet of the curved channel and were tracked while they were traveling along the channel.

In addition to the dynamic forces caused by the flow itself, the effect of wall-induced lift forces for all surrounding walls was considered during the simulation. Moreover, the drag force within the entire volume of the chip was calculated under the Stokes Drag law option

within the software. It is due to the fact that in low flow rates, microfluidic systems operate in the Stokes Flow regime, in which viscous forces are dominant compared to inertial forces.

As shown in Figure 14, a coarser mesh size was selected for this analysis, resulting in a decent resolution in the sharp corners and transition points. Moreover, it lowers the run time for the simulation which is advantageous considering the limitation on the computation power of the device used for this simulation. Additionally, to further simplify the geometry, this section of the microfluidic device was modeled and analyzed as sole device separated from rest of the microfluidic chip.

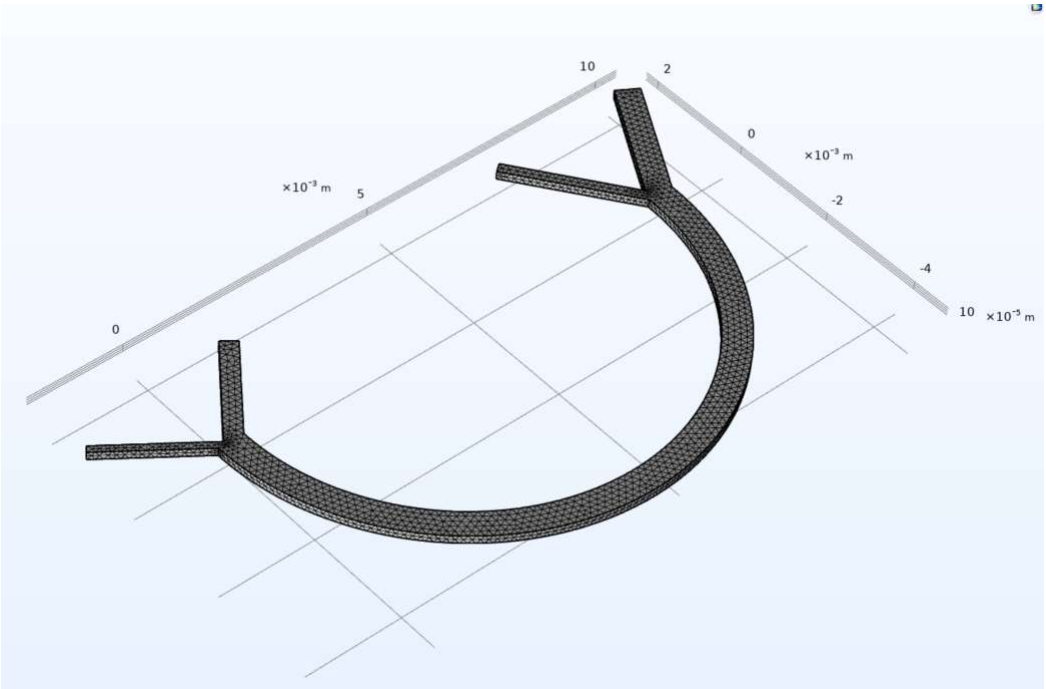

Figure 14: The modified design for an efficient separation

The obtained result is shown in the figure 15 that illustrates despite all three particles being initially released from the same inlet at the entry of the curved section of the microfluidic chip, further downstream, the smaller particles got separated from the larger one due to their inertia and become inclined towards the convex wall (inner wall).

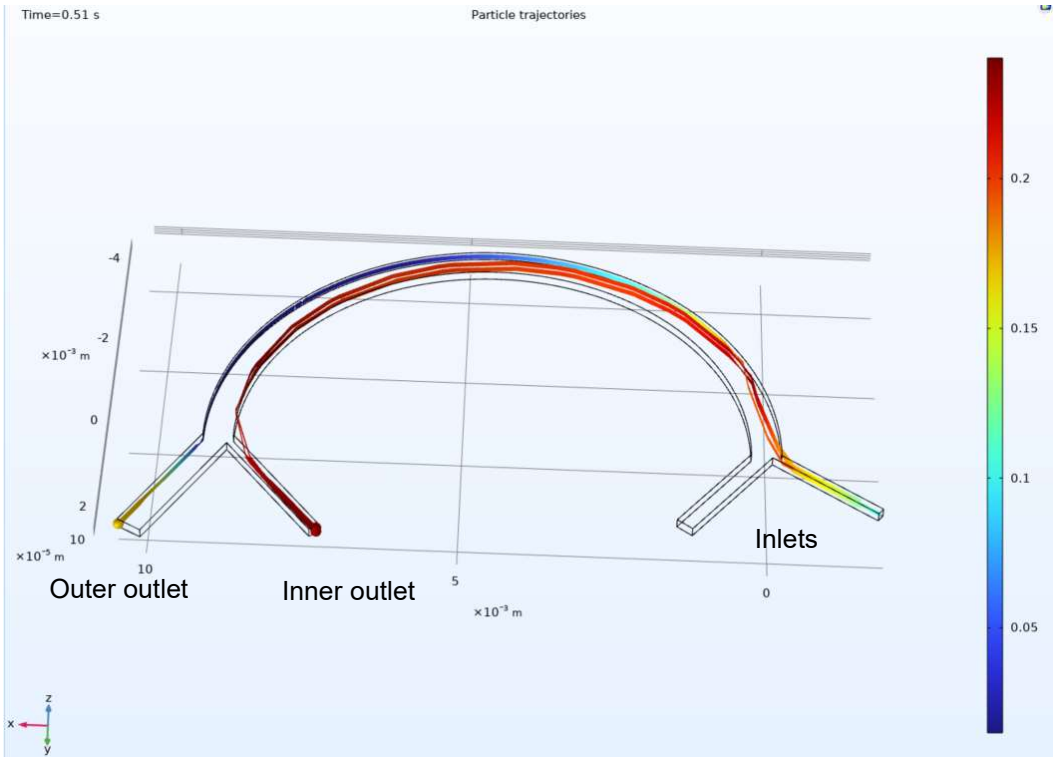

Figure 15: Inertial separation of the floating particles

The scale bar in Figure 15 shows the particles' speed (m/s). As expected, larger particles (20 um) travel slower along the microchannel compared to smaller ones and exit through the outer outlet.

Chapter 3. Discussion

3.1. Discussion

The present project introduces a microfluidic device integrated with SERS for continuous, real-time characterization of microplastics. The suggested microfluidic chip has a relatively simple geometry including a flat structure which offers ample advantages over sophisticated designs as it is easier to fabricate with a lower scrap rate. It mixes the sample that contains microplastics with a buffer such as PBS and then by passing the mixture through an array of consecutive expansion and contraction zones, initiates a secondary flow within the main flow. This secondary flow focuses the microplastics in the middle of the channel and makes them ready to get scanned by SERS laser beam. Silver nanoparticle (NPs) is suggested for this method since it has been reported to create a higher shift in Raman spectrum and yield in a

According to the research work done by Lee et al. [35] there is an optimum number of expansion and contraction zones that would bring the particles in the middle of the channel. The microfluidic device introduced in this project is inspired from that research work and utilized the same geometry and results in order to achieve perfect focusing of the particles in the middle of the microchannels.

Afterwards, the microchannel turns into a spiral channel in order to create dean flow and separate floating particles and provides opportunity of further analysis on the particles in the downstream by bifurcating them into multiple sub microchannels. Simulation results

of the second design done by COMSOL Multiphysics agrees with the Dean Cycle concept introduced by Hou et al. [40] as it showed that in a 630˚ spiral, the smaller particle (with the size of 6 and 10μ) after 180˚ of the spiral moves toward the opposite side wall of the channel. However, as it goes further downstream at around 630˚, they tends to return towards the concave wall (outer wall). Therefore, to have an efficient separation of the particles, the bifurcation was designed to occur at around 180˚ where the largest particle (20um) can be separated. Using the same technique the other two particles, and in general particles of any size can be separated further down the spiral.

3.2. Future work

In this project only three different sizes of particle are studied, and the microfluidic device is engineered based on obtained results. However, in real world examples microplastics can vary in size up to a few millimeters. In case of having access to a more powerful computing tool, a more extensive analysis can be done in at attempt to cover a wider range of microplastic particles. In addition, fabricating the suggested microfluidic device can be assumed as a proof of functionality and efficiency.

References

1. Robert C. Hale, Meredith E. Seeley, Mark J. La Guardia, Lei Mai, Eddy Y. Zeng, "A Global Perspective on Microplastics", JGR Oceans, Volume 125, Issue 1, January 2020, doi:10.1029/2018JC014719

2. Anthony L. Andrady, "Microplastics in the marine environment", Marine Pollution Bulletin, Volume 62, Issue 8, August 2011, Pages 1596-1605, doi:10.1016/j.marpolbul.2011.05.030

3. Marcus Eriksen, Laurent C. M. Lebreton, Henry S. Carson, Martin Thiel, Charles J. Moore, Jose C. Borerro, Francois Galgani, Peter G. Ryan, Julia Reisser, "Plastic Pollution in the World's Oceans: More than 5 Trillion Plastic Pieces Weighing over 250,000 Tons Afloat at Sea", PLOS ONE, doi:10.1371/journal.pone.0111913

4. Jing Sun, Zitong Peng, Zhuo-Ran Zhu, Weng Fu, Xiaohu Dai, Bing-Jie Ni, "The atmospheric microplastics deposition contributes to microplastic pollution in urban waters", Water Res., October 2022, doi:10.1016/j.watres.2022.119116.

5. Napper IE, Thompson RC, "Release of synthetic microplastic plastic fibres from domestic washing machines: Effects of fabric type and washing conditions", Mar Pollut Bull., 2016 Nov, doi: 10.1016/j.marpolbul.2016.09.025.

6. Md Shahriar Mahbub, Mehnaz Shams, "Acrylic fabrics as a source of microplastics from portable washer and dryer: Impact of washing and drying parameters", Science of The Total Environment, Volume 834, 2022, doi.org/10.1016/j.scitotenv.2022.155429.

7. Cole M, Lindeque P, Fileman E, Halsband C, Goodhead R, Moger J, Galloway TS, "Microplastic ingestion by zooplankton", Environ Sci Technol, 2013 Jun, doi: 10.1021/es400663f.

8. Garnier Y, Jacob H, Guerra AS, Bertucci F, Lecchini D, "Evaluation of microplastic ingestion by tropical fish from Moorea Island, French Polynesia" Mar Pollut Bull., 2019 Mar, doi: 10.1016/j.marpolbul.2019.01.038.

9. Lee J, Hong S, Song YK, Hong SH, Jang YC, Jang M, Heo NW, Han GM, Lee MJ, Kang D, Shim WJ, "Relationships among the abundances of plastic debris in different size classes on beaches in South Korea", Mar Pollut Bull., 2013 Dec, doi: 10.1016/j.marpolbul.2013.08.013.

10. Hidalgo-Ruz V, Thiel M, "Distribution and abundance of small plastic debris on beaches in the SE Pacific (Chile): a study supported by a citizen science project", Mar Environ Res., 2013 Jun-Jul, doi: 10.1016/j.marenvres.2013.02.015.

11. Napper, Imogen & Wright, Luka Seamus & Barrett, Aaron & Parker-Jurd, Florence, Thompson Richard, "Potential microplastic release from the maritime industry: Abrasion of rope", Science of The Total Environment, doi: 10.1016/j.scitotenv.2021.150155.

12. Yang, R., Mei, L., Fan, Y., "Fabrication of liquid cell for in situ transmission electron microscopy of electrochemical processes", Nat Protoc 18, 2023, doi.org/10.1038/s41596-022-00762-y

13. Cooper DA, Corcoran PL, "Effects of mechanical and chemical processes on the degradation of plastic beach debris on the island of Kauai, Hawaii", Mar Pollut Bull. 2010 May, doi: 10.1016/j.marpolbul.2009.12.026.

14. Desforges JP, Galbraith M, Dangerfield N, Ross PS, "Widespread distribution of microplastics in subsurface seawater in the NE Pacific Ocean", Mar Pollut Bull., 2014 Feb, doi: 10.1016/j.marpolbul.2013.12.035.

15. A. Vianello, A. Boldrin, P. Guerriero, V. Moschino, R. Rella, A. Sturaro, L. Da Ros, "Microplastic particles in sediments of Lagoon of Venice, Italy: First observations on occurrence, spatial patterns and identification", Estuarine, Coastal and Shelf Science, Volume 130, 2013, doi.org/10.1016/j.ecss.2013.03.022.

16. Löder M.G.L.,Gerdts G., "Methodology Used for the Detection and Identification of Microplastics—A Critical Appraisal", Marine Anthropogenic Litter, Heidelbderg, Germany, Springer Open, pp.201-227. doi:0.1007/978-3-319-16510-3_8

17. Van Cauwenberghe L, Vanreusel A, Mees J, Janssen CR, "Microplastic pollution in deep-sea sediments", Environ Pollut., 2013 Nov, doi: 10.1016/j.envpol.2013.08.013.

18. Collard F, Gilbert B, Eppe G, Parmentier E, Das K, "Detection of Anthropogenic Particles in Fish Stomachs: An Isolation Method Adapted to Identification by Raman Spectroscopy", Arch Environ Contam Toxicol, 2015 Oct, doi: 10.1007/s00244-015-0221-0.

19. Nathan G. Greeneltch, Martin G. Blaber, George C. Schatz, Richard. P. Van Duyne, "The Journal of Physical Chemistry, 2013, doi: 10.1021/jp310846j

20. M. Fleischmann, P.J. Hendra, A.J. McQuillan, “Raman spectra of pyridine adsorbed at a silver electrode”, Chemical Physics Letters, Volume 26, Issue 2, 1974, Pages 163-166, SSN 0009-2614, doi:10.1016/0009-2614(74)85388-1.

21. David L. Jeanmaire, Richard P. Van Duyne, “Surface raman spectroelectrochemistry: Part I. Heterocyclic, aromatic, and aliphatic amines adsorbed on the anodized silver electrode”, Journal of Electroanalytical Chemistry and Interfacial Electrochemistry, Volume 84, Issue 1, 1977, Pages 1-20, ISSN 0022-0728, doi:10.1016/S0022-0728(77)80224-6.

22. M. Grant Albrecht, J. Alan Creighton, "Anomalously intense Raman spectra of pyridine at a silver electrode", Journal of the American Chemical Society, Vol 99/Issue 15, June 1977, doi:10.1021/ja00457a071

23. Patanjali Kambhampati, C. M. Child, Michelle C. Foster, Alan Campion, "On the chemical mechanism of surface enhanced Raman scattering: Experiment and theory", Journal of chemical physics, March 1998, doi:10.1063/1.475909

24. Sebastian Schlücker, "Surface-Enhanced Raman Spectroscopy: Concepts and Chemical Applications", Angewandte chemie international eddition, April 2014, doi:10.1002/anie.201205748

25. Rajapandiyan Panneerselvam, Guo-Kun Liu, Yao-Hui Wang, Jun-Yang Liu, Song-Yuan Ding, Jian-Feng Li, De-Yin Wu, Zhong-Qun Tian, "Surface-enhanced Raman spectroscopy: bottlenecks and future directions", Royal society of chemistry, October 2017, doi: 10.1039/C7CC05979E

26. Ye Zhang, Shaojie Zhao, Jinkai Zheng, Lili He, "Surface-enhanced Raman spectroscopy (SERS) combined techniques for high-performance detection and characterization", TrAC Trends in Analytical Chemistry, Volume 90, 2017, doi:10.1016/j.trac.2017.02.006.

27. Lv L, He L, Jiang S, Chen J, Zhou C, Qu J, Lu Y, Hong P, Sun S, Li C, "In situ surface-enhanced Raman spectroscopy for detecting microplastics and nanoplastics in aquatic environments", Sci Total Environ, 2020 Aug, doi: 10.1016/j.scitotenv.2020.138449

28. Katrin Kneipp, Harald Kneipp, Irving Itzkan, Ramachandra R. Dasari, and Michael S. Feld, "Ultrasensitive Chemical Analysis by Raman Spectroscopy", Chemical Reviews, 1999, doi: 10.1021/cr980133

29. Sara Abalde-Cela, Paula Aldeanueva-Potel, Cintia Mateo-Mateo, Laura Rodríguez-Lorenzo, Ramón A. Alvarez-Puebla, Luis M. Liz-Marzán, "Surface-enhanced Raman scattering biomedical applications of plasmonic colloidal particles",journal of the royal society interface, May 2010, doi: 10.1098/rsif.2010.0125.focus

30. Dino Do Carlo, "Inertial microfluidics", Lab on a chip, June 2009, doi:10.1039/B912547G

31. Ali Asgar S. Bhagat, Sathyakumar S. Kuntaegowdanahalli, Ian Papautsky, "Enhanced particle filtration in straight microchannels using shear-modulated inertial migration", Physics of fluids, Volume 20, Issue 10, October 2008, doi: 10.1063/1.2998844

32. Joseph M. Martel, Mehmet Toner, "Inertial Focusing in Microfluidics", ANNUAL REVIEW OF BIOMEDICAL ENGINEERING Volume 16, 2014, doi:10.1146/annurev-bioeng-121813-120704

33. Jian Zhoua, Ian Papautsky, "Fundamentals of inertial focusing in microchannels",Lab on a chip, Issue 6, January 2013, doi: 10.1039/C2LC41248A

34. Jian Zhou, Premkumar Vummidi Giridhar, Susan Kasperb, Ian Papautsky, "Modulation of aspect ratio for complete separation in an inertial microfluidic channel", Lab on a chip, Issue 10, March 2013, doi: 10.1039/C3LC50101A

35. Myung Gwon Lee, Sungyoung Choi, Je-Kyun Park, "Three-dimensional hydrodynamic focusing with a single sheath flow in a single-layer microfluidic device", Lab on a chip, Issue 21, August 2009, doi: 10.1039/B910712F

36. Warkiani ME, Khoo BL, Wu L, Tay AK, Bhagat AA, Han J, Lim CT, "Ultra-fast, label-free isolation of circulating tumor cells from blood using spiral microfluidics", Nature Protocol, 2016 Jan, doi: 10.1038/nprot.2016.003.

37. Dean, W. R., "XVI. Note on the motion of fluid in a curved pipe", The London, Edinburgh, and Dublin Philosophical Magazine and Journal of Science, doi: 10.1080/14786440708564324

38. Shinichi Ookawara, David Street, Kohei Ogawa, "Numerical study on development of particle concentration profiles in a curved microchannel", Chemical Engineering Science, Volume 61, Issue 11, 2006, doi:10.1016/j.ces.2006.01.016.

39. Peter B. Howell, David R. Mott, Joel P. Goldena, Frances S. Ligler, "Design and evaluation of a Dean vortex-based micromixer", Lab on a chip, Issue 6, November 2004, doi:10.1039/B407170K

40. Han Wei Hou, Majid Ebrahimi Warkiani, Bee Luan Khoo, Zi Rui Li, Ross A. Soo, Daniel Shao-Weng Tan, Wan-Teck Lim, Jongyoon Han, Ali Asgar S. Bhagat, Chwee Teck

Lim, "Isolation and retrieval of circulating tumor cells using centrifugal forces", Sci Rep 3, 1259 (2013), doi: 10.1038/srep01259

41. Wei Yu, Xiangdong Liu, Bo Li, Yongping Chen, "Experiment and prediction of droplet formation in microfluidic cross-junctions with different bifurcation angles", International Journal of Multiphase Flow, Volume 149, 2022, doi: 10.1016/j.ijmultiphaseflow.2022.103973.

42. Scott J. Hymel, Hongzhi Lan, Hideki Fujioka, Damir B. Khismatullin, "Cell trapping in Y-junction microchannels: A numerical study of the bifurcation angle effect in inertial microfluidics", Physics of fluids, Volume 31, Issue 8, August 2019, doi: 10.1063/1.5113516